Original Article

MOLECULAR METABOLISM

Hypothalamic *Irak4* is a genetically controlled regulator of hypoglycemia-induced glucagon secretion

Alexandre Picard [1], Xavier Berney [1], Judit Castillo-Armengol [1,2], David Tarussio [1], Maxime Jan [1], Ana Rodriguez Sanchez-Archidona [1], Sophie Croizier [1], Bernard Thorens [1,*]

ABSTRACT

Objectives: Glucagon secretion to stimulate hepatic glucose production is the first line of defense against hypoglycemia. This response is triggered by so far incompletely characterized central hypoglycemia-sensing mechanisms, which control autonomous nervous activity and hormone secretion. The objective of this study was to identify novel hypothalamic genes controlling insulin-induced glucagon secretion.
Methods: To obtain new information on the mechanisms of hypothalamic hypoglycemia sensing, we combined genetic and transcriptomic analysis of glucagon response to insulin-induced hypoglycemia in a panel of BXD recombinant inbred mice.
Results: We identified two QTLs on chromosome 8 and chromosome 15. We further investigated the role of *Irak4* and *Cpne8*, both located in the QTL on chromosome 15, in C57BL/6J and DBA/2J mice, the BXD mouse parental strains. We found that the poor glucagon response of DBA/2J mice was associated with higher hypothalamic expression of *Irak4*, which encodes a kinase acting downstream of the interleukin-1 receptor (Il-1R), and of *Il-ß* when compared with C57BL/6J mice. We showed that intracerebroventricular administration of an Il-1R antagonist in DBA/2J mice restored insulin-induced glucagon secretion; this was associated with increased c-fos expression in the arcuate and paraventricular nuclei of the hypothalamus and with higher activation of both branches of the autonomous nervous system. Whole body inactivation of *Cpne8,* which encodes a Ca^{++}-dependent regulator of membrane trafficking and exocytosis, however, had no impact on insulin-induced glucagon secretion.
Conclusions: Collectively, our data identify *Irak4* as a genetically controlled regulator of hypoglycemia-activated hypothalamic neurons and glucagon secretion.

Keywords Genetic screening; Insulin-induced hypoglycemia; Hypothalamus; Glucagon; Autonomous nervous system

1. INTRODUCTION

The brain mostly relies on glucose as a source of metabolic energy. Hence, homeostatic glucoregulatory mechanisms are needed to maintain blood glucose at the minimum level of ∼5 mM to ensure sufficient glucose availability to the brain [1]. Hypoglycemia-sensing cells located in the central nervous system and in the periphery, e.g., in the hepatoportal vein and in the carotid bodies, initiate a counterregulatory response (CRR) when the blood glucose level falls below the euglycemic level [2–4]. CRR involves the activation of the autonomous nervous system and the hypothalamo-pituitary-adrenal axis by the brain, leading to the secretion of glucagon by pancreatic alpha cells and of catecholamines and glucocorticoids by the adrenal glands [4]. This promotes hepatic neoglucogenesis, stimulates lipolysis, and inhibits insulin secretion as well as glucose uptake by muscle and fat. This coordinated response restores euglycemia to preserve sufficient glucose provision to the brain. While the CRR prevents hypoglycemia in healthy individuals, this response becomes progressively blunted in type 1 and insulin-treated type 2 diabetic patients, leading to recurrent hypoglycemic episodes of increasing severity, a condition known as hypoglycemia-associated autonomic failure (HAAF), which represents a major limitation in the insulin-based therapy of diabetes [5].

In the brain, glucose sensing neurons have been identified in the hypothalamus and in the brainstem [6,7], and they are commonly classified in two categories depending on their activation by a rise (glucose excited, GE) or a fall in blood glucose concentration (glucose inhibited, GI) [7–9]. In the brainstem, glucose-sensing neurons are found in the dorsal vagal complex (DVC) composed of the area postrema (AP), the nucleus of the solitary tract (NTS) and the dorsal motor nucleus of the vagus (DMNX) [6]. In the hypothalamus, glucose-sensing neurons are distributed in the arcuate (ARH), the paraventricular (PVN), the lateral (LH), the dorsomedial (DMH), and the ventromedial hypothalamic nuclei (VMN) [6]. Among these nuclei, the VMN has been extensively studied for its implication in glucose sensing and in the control of glucagon secretion [10–13]. Glucose sensing by GE neurons has been proposed to depend on a Glut/glucokinase/K_{ATP} channel signaling pathway similar to that controlling glucose-stimulated insulin secretion in pancreatic β cells [14–18]. However,

[1]Center for Integrative Genomics, University of Lausanne, 1015, Lausanne, Switzerland [2]Novo Nordisk A/S, Måløv, Denmark

*Corresponding author. Center for Integrative Genomics, University of Lausanne, CH-1015, Lausanne, Switzerland. Fax: +41 21 692 3985. E-mail: bernard.thorens@unil.ch (B. Thorens).

Received February 14, 2022 • Revision received March 16, 2022 • Accepted March 17, 2022 • Available online 24 March 2022

https://doi.org/10.1016/j.molmet.2022.101479

glucose sensing by GE neurons of the VMN is not suppressed when the glucokinase gene is inactivated [19] and the Na^+/glucose co-transporters SGLT1 and SGLT3 are required for glucose sensing by specific populations of GE neurons [20]. Activation of GI neurons firing by hypoglycemia requires activation of AMP-activated protein kinase [21–23] and the regulated activity of CFTR [24], anoctamine 4 [25], two-pore-domain K^+ channels [26], or the Na^+/K^+ATPase [27,28]. Thus, the mechanisms of neuronal glucose sensing are diverse and are still incompletely understood.

Unbiased identification of genes involved in the CRR and its deregulation is of significant physiological and pathophysiological interest. Such identification is possible by screening genetic reference populations for quantitative trait loci controlling glucagon secretion. The BXD mice consist of a large panel of recombinant inbred lines derived from the cross of C57BL/6J and DBA/2J mice [29]. In a previous study, we screened a panel of 36 BXD mouse lines to identify QTLs controlling neuroglucopenia (2-deoxy-D-glucose, 2DG)-induced glucagon secretion. This led to the identification of a QTL on chromosome 7 and of *Fgf15* produced by DMH neurons, as a negative a regulator of glucagon secretion but a positive inducer of hepatic glucose production through direct activation of sympathetic nervous activity [30,31].

Here, we performed a new screening aimed to discover hypothalamic genes controlling glucagon secretion in response to insulin-induced hypoglycemia, as this may be more relevant to the condition of insulin-induced HAAF. This led to the identification of two QTLs, one on chromosome 8 and the second one on chromosome 15. We then searched for candidate genes in these QTL based on the assumption that they were expressed in the hypothalamus and that their level of expression correlated with the glucagon trait. *Irak4*, encoding a protein kinase acting downstream of the Il-1R and Toll-like receptor (TIR) signaling pathway [32], was found to be the best candidate on chromosome 15. Physiological studies showed that high *Irak4* as well as *Il-1ß* expression in the hypothalamus of DBA/2J mice were responsible for the low hypoglycemia-induced glucagon response observed in these mice.

2. RESEARCH DESIGN AND METHODS

2.1. Mice

BXD mice (see list of the strains used in Supplemental Table 1) were purchased from the Jackson Laboratory (Bar Harbor, Maine, USA). C57BL/6J and DBA/2J mice were purchased from Charles River Laboratories (Saint Germain Nuelles, France). Mice were housed on a 12-h light/dark cycle and fed a standard rodent chow diet (Diet 3436, Provimi Kliba AG, Kaiseraugst, Switzerland). Experiments were performed with 8- to 12-week-old male mice. All animal experimentations were approved by the Veterinary Office of Canton de Vaud under license agreement VD 3363.

2.2. Biochemical measurements

Blood was collected from the submandibullary (glucagon) or tail veins (glycemia). Glycemia was measured using a glucometer (Ascensia Breeze 2, Bayer Healthcare, Lerverkusen, Germany). ELISA was used to quantify plasma glucagon (cat. number:10-1271-01, Mercodia, Uppsala, Sweden). Pancreatic glucagon content was determined as described previously [31].

2.3. Phenotyping of insulin-induced glucagon secretion in BXD mice and their parental strains

Insulin-induced glucagon secretion was assessed in 5 mice for each of the 36 BXD lines and in the parental C57BL/6J and DBA/2J strains. Mice were handled daily for two weeks before the experiments. Before the first experiment, mice were fasted for 6 h, and glycemia was measured at 2:00 p.m. The mice then received an i.p. injection of NaCl 0.9%. Blood was collected 1 h later for basal glucagon quantification. Mice were then allowed to recover for two weeks with daily handling. The same protocol was used with i.p. injection of insulin (Actrapid, Novo Nordisk Pharma, 0.8 U/kg).

2.4. QTL and eQTL mapping

QTL and eQTL mappings were performed using the R package R/qtl as previously described [31,33]. QTL interval mapping was calculated using the expected-maximization algorithm, a 5% genotyping error rate, and pseudomarkers were generated every cM. QTL location was obtained with 1.5 LOD score (equivalent to 6.915 likelihood ratio statistics (LRS)) support intervals as suggested [34]. Significant QTLs were determined for each trait using 5% false discovery rate threshold estimated from 1000 permutations.

2.5. RNA-Seq analysis

RNA-Seq from pools of 3–6 hypothalami of 12-week-old BXD mice had been previously generated [31]. Read counts were normalized in transcripts per million (TPM), and Pearson's correlations were calculated between gene expression levels and physiological traits. RNA-Seq data are accessible *via* GEO under accession number GSE87586.

2.6. I.c.v. cannulation

Surgeries were performed under ketamine/xylazine anesthesia. Cannulas were placed in the lateral ventricle (−0.7 mm from the Bregma; −1.3 mm from the midline; −2.0 mm from the surface of the skull) [35]. The animals were allowed to recover for one week before experiment with daily handling and body weight monitoring.

2.7. I.c.v. injections

At 1:00 p.m. on the test day, mice received either an i.c.v. injection of saline or Anakinra (50 µg; Kineret®, recombinant human IL-1ra, Swedish Orphan Biovitrum AB) in a total volume of 5 µL. One hour later, mice were injected i.p. with saline or 0.8 U/kg of insulin. Blood was collected 1 h later for glucagon quantification, and the brains were fixed 2 h later for immunofluorescence detection of c-fos.

2.8. Physiological measurements

Insulin-induced hypoglycemia tests (Actrapid, 0.8 U/kg) were performed in 6-h food-deprived mice injected i.c.v. with NaCl 0.9% or Anakinra 1 h before i.p. injection of NaCl 0.9% or 0.8 U/kg insulin. Glycemia was measured before i.c.v. and i.p. injections and 1 h after i.p. injections. Blood was collected for glucagon measurement 1 h after the i.p. injections. Hyperinsulinemic-hypoglycemic clamps were performed as previously described [36]. Briefly, 6 h-fasted C57BL/6J and DBA/2J mice received at 2:00 p.m. on the test day either i.c.v. NaCl 0.9% or Anakinra (50 µg) at the start of the clamp procedure. After 90 min and after at least 30 min of stable glucose infusion rates and glycemia, blood was sampled to quantify plasma glucagon.

2.9. Immunofluorescence microscopy

C-fos immunodetection was performed in C57BL/6J that received i.p. injection of saline or insulin 0.8 U/kg, and in DBA/2J mice that received an i.c.v. injection of saline or Anakinra 1 h before an i.p. injection of insulin 0.8U/kg. Two hours later, the mice were fixed by cardiac perfusion of 4% cold paraformaldehyde (PFA) in sodium phosphate buffer (0.1 M, pH 7.4). Brains were then dissected and kept for 2 h in PFA at 4 °C, incubated overnight in a 20% sucrose solution at 4 °C,

and frozen at −80 °C. Serial 25-μm-thick hypothalamic cryosections were prepared and incubated first for 1 h in 0.1M phosphate buffer pH 7.4 containing 4% normal goat serum and 0.3% Triton X-100 and then for 24 h at room temperature with rabbit monoclonal antibodies against c-fos (cat. number: 2250, 1/1000, Cell Signaling, Danvers, USA) and for 2 h at room temperature with Alexa Fluor 488- or 568-conjugated goat anti-rabbit IgG antibodies (cat. number: 11008, 1/500, Life Technologies, Carlsbad, USA). Nuclei were counterstained with DAPI (cat. number: D9542, Sigma Aldrich, St. Louis, USA), and the slides were mounted in Mowiol (cat. number: 81381, Sigma Aldrich, St. Louis, USA).

Images were acquired with a Zeiss Axio Imager D1 microscope interfaced with Axiovision software equipped with ApoTome.2 and a Camera Axiocam 702 mono (Zeiss, Oberkochen, Germany). The number of c-fos-positive cells in the ARH and PVN was normalized to the respective surface of each nuclei using Image J software.

2.10. In situ hybridization

For *in situ* hybridization detection of *Irak4* based on Atto 550 fluorescence, brains of C57BL/6J and DBA/2J mice were dissected as described above for c-fos immunodetection. Twenty-five micrometer hypothalamic cryosections were then prepared, and *in situ* hybridization was performed using Advanced Cell Diagnostics probes (cat. number: 444451) and RNAscope Fluorescent Multiplex Detection Reagents (Advanced Cell Diagnostics, Newark, USA) following the manufacturer's instructions. *Irak4* mRNA spots were quantified using ImageJ software on 2 hemisections between the Bregma −0.82 and −0.94 mm for the PVN and −1.70 to 1.82 mm for the ARH on 4 to 5 animals per group. The number of spots was then normalized to the respective surface of each nucleus.

2.11. Autonomous nervous system activity recording

Unipolar parasympathetic and sympathetic activities were recorded along the carotid artery as previously described [30,31]. Recordings were performed for 1.5 h under isoflurane anesthesia (30 min during basal condition after i.c.v. NaCl 0.9%/Anakinra and before i.p. insulin 0.8 U/kg, 1 h during insulin-induced hypoglycemia) using the LabChart 8 software (AD Instrument, Oxford, UK). Data were digitized with PowerLab 16/35 (AD Instrument, Oxford, UK). Signals were amplified 10^5 times and filtered using a 100/1000 Hz band pass filter. Firing rate analysis was performed using the LabChart 8 software.

2.12. Statistical analysis

Data are expressed as mean ± SEM. Statistical analysis was performed using GraphPad Prism® 9.1.0, either by a mixed-effects analysis followed by a Sidak's post hoc test, a repeated-measures two-way ANOVA followed by a Sidak's post hoc test, or by an unpaired two-tailed Student's t-test. P-values of <0.05 were considered to be significant.

3. RESULTS

3.1. Identification of QTLs for insulin-induced glucagon secretion

To search for the loci controlling hypoglycemia-induced glucagon secretion, we performed a genetic screening of a panel of 36 BXD mouse lines and their parental C57BL/6J and DBA/2J strains. In the first experiment, five mice from each line were fasted for 6 h and then injected intraperitoneally (i.p.) with a saline solution. Blood was collected 1 h later for plasma preparation and glucagon measurement. The experiment was repeated two weeks later, but mice received i.p. injections of 0.8 U/kg insulin instead of saline to induce hypoglycemia. Plasma glucagon levels after saline injections were in the same low range for all the mouse lines tested but varied markedly between lines upon insulin-induced hypoglycemia (Figure 1A). The glucagon response was not correlated with the pancreas glucagon content of the BXD lines (Figure 1B); it was, however, correlated with the level of insulin-induced hypoglycemia (Figure 1C) and varied up to 23-fold when compared with BXD 70 (7.2 pM) and BXD 98 (169.2 pM) (Figure 1 D). The plasma glucagon data of Figure 1D were then used for QTL mapping and led to the identification of two genome-wide significant QTLs on chromosome 8 (LRS = 19.23) and on the distal part of chromosome 15 (LRS = 26.27) (Figure 1E). As the glucagon response showed a strong correlation with the hypoglycemia levels, the identified QTLs may also control insulin sensitivity. We thus performed a QTL analysis for insulin-induced hypoglycemia. This led to the identification of a single QTL on chromosome 8 (Figure 1F), located in the same genomic interval as the glucagon QTL. This region may thus influence both insulin sensitivity and hypoglycemia-induced glucagon secretion. This result also indicated that the QTL on chromosome 15 was related to glucagon secretion rather than to insulin sensitivity.

The QTL on chromosome 8 spans ∼6.38 Mb between markers rs13479624 and rs33450716 with a peak LRS on rs13479628 (Figure 2A). This QTL contains 155 genes and explains 41.4% of the variance of the trait. To identify candidate genes in the QTL controlling insulin-induced glucagon secretion, we postulated that they must be expressed in the hypothalamus and that their expression level correlated to the insulin-induced glucagon secretion trait. We then analyzed the transcriptomic data from the hypothalamus of naïve BXD and their parental strains that we previously generated [31]. Of the 155 genes present in this locus, the level of expression of 3 of them was significantly correlated to the trait, named *261005L07Rik*, *Agpat5*, and *LOC547150* (figure 2B).

The QTL on the chromosome 15 spans ∼4.94 Mb between pseudomarker c15.loc87 and marker rs13482723 with a peak LRS on rs3685284 (Figure 3A). This QTL contains 42 genes and explains 51.8% of the variance of the trait. Forty-two genes are present in this locus, and the expression level of 8 of them was significantly correlated with the glucagon trait (Figure 3B). The most strongly correlated genes were *Irak4* ($r = -0.584$; $p = 1.0 \times 10^{-4}$) and *Tmem117* ($r = -0.553$; $p = 3.0 \times 10^{-4}$) (Figure 3B and C). The correlation of the other 6 genes with insulin-induced glucagon secretion showed at least 10-fold less significant p-values. We found that a cis eQTL between markers rs3685284 and rs45781537 with peak LRS = 40.6 on rs13482723 controls the expression levels of *Irak4* (Figure 3D) and that the presence of the DBA/2J allele at rs13482723 in BXD mice led to higher hypothalamic *Irak4* expression than the presence of the C57BL/6J allele (Figure 3E). Thus, the same genomic interval on chromosome 15 controls both hypothalamic *Irak4* expression and insulin-induced glucagon secretion.

Because *Irak4* showed the strongest, negative correlation with the glucagon secretion trait, we further examined its role in the response to hypoglycemia. The physiological roles of *Tmem117* and *Agapt5* in insulin-induced glucagon will be published separately. Here, we will also report on the role of *Cpne8* encoding a calcium- and lipid-binding protein present in the QTL of chromosome 15 [37].

3.2. Hypothalamic Irak4 and insulin-induced glucagon secretion

The *Irak4* (interleukin-1 receptor-associated kinase 4) gene encodes a 459-amino-acid protein kinase. It acts downstream of Il-1R and TIRs to activate an inflammatory response *via* the NF-κB and MAPK signaling pathways [32,38]. In DBA/2J mice, the *Irak4* gene

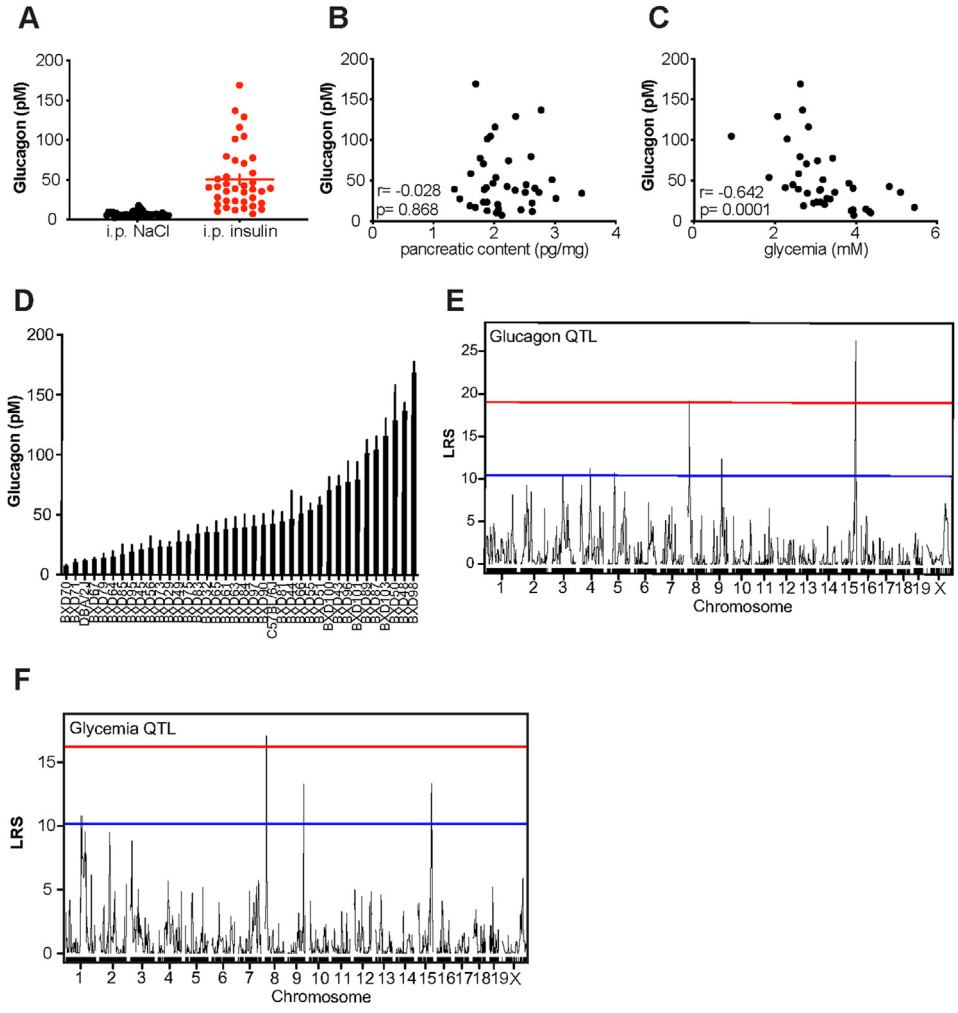

Figure 1: Identification of QTLs controlling hypoglycemia-induced glucagon secretion. A: Basal and hypoglycemia-induced glucagon secretion in the 36 BXD lines and the parental C57BL/6J and DBA/2J strains. Each circle represents the mean glucagonemia for each strain. B: Scatterplot of the correlation between plasma glucagon levels and total pancreas glucagon content for all the mouse lines tested. C: Scatterplot of the correlation between plasma glucagon levels and glycemia for all the mouse lines tested. D: Plasma glucagon levels 1 h after i.p. insulin injection in the indicated BXD lines and the parental strains. E: Whole genome significant QTLs on chromosome 8 and 15. The red line indicates the whole genome significant threshold ($p \leq 0.05$). The blue line indicates the whole genome suggestive threshold ($p \leq 0.63$). F: Whole genome significant QTL on chromosome 8 for glycemia 1 h after i.p. insulin injection. The red line indicates the whole genome significant threshold ($p \leq 0.05$). The blue line indicates the whole genome suggestive threshold ($p \leq 0.63$).

sequence shows two missense variants as compared to the C57BL/6J gene, namely I11V and N183R [39,40]. These variants are located outside of the functional domains of Irak4 and are not predicted to modify its function (https://www.uniprot.org/uniprot/Q8R4K2) [41]. Analysis of the level of expression of genes that pertain to the Il-1β and TIR signaling pathways (Table 1) showed that *Irak4* was expressed at a higher level (log-fold change (LogFC) = 0.689) in the hypothalamus of DBA/2J mice as compared to that of C57BL/6J mice. We also found higher expression in DBA/2J of *Il-1β* (LogFC = 2.524) and of *Tlr6* (LogFC = 1.399), a receptor that recognizes pathogen-associated molecular patterns.

To identify hypothalamic sites activated by insulin-induced hypoglycemia, where Irak4 expression levels would direct the differential glucagon response of C57Bl/6J and DBA/2J mice, we analyzed c-fos expression 2 h after i.p. saline or insulin injections in C57BL/6J mice. Figure 4A–D shows that hypoglycemia strongly induced c-fos expression in the ARH and the PVN. We thus analyzed the expression level of *Irak4* by *in situ* hybridization in these hypothalamic nuclei. We found that *Irak4* was expressed at a 2.5-fold higher level in the ARH, but not the PVN of DBA/2J mice as compared to C57BL/6J mice (Figure 4E–J).

DBA/2J mice secrete markedly less glucagon upon insulin-induced hypoglycemia as compared to C57BL/6J mice (11.9 ± 0.84 pM vs. 42.6 ± 10.99 pM for DBA/2J vs. C57BL/6J mice, respectively) (Figure 1B) despite reaching similar hypoglycemic levels (4.3 ± 0.28 mM vs 4.8 ± 0.20 mM for DBA/2J and C57BL/6J mice, respectively). Thus, the higher expression of *Irak4,* especially in the ARH, and of *Il-1β* in the hypothalamus of DBA/2J mice suggested that the Il-1β/Irak4 signaling pathway could regulate insulin-induced glucagon secretion. To test this hypothesis, we evaluated the effect of blocking hypothalamic Il-β signaling on glucagon secretion. C57BL/6J and DBA/2J mice were injected i.c.v. with saline or the Il-1R antagonist Anakinra followed 1 h later by an i.p. injection of saline or insulin, and blood was collected after 60 min for plasma glucagon measurements. In C57BL/6J mice, i.c.v. injection of Anakinra had no effect on glycemia after i.p. saline (Figure 5A) or i.p. insulin injections (Figure 5B), and glucagon secretion increased to the same extent in

A

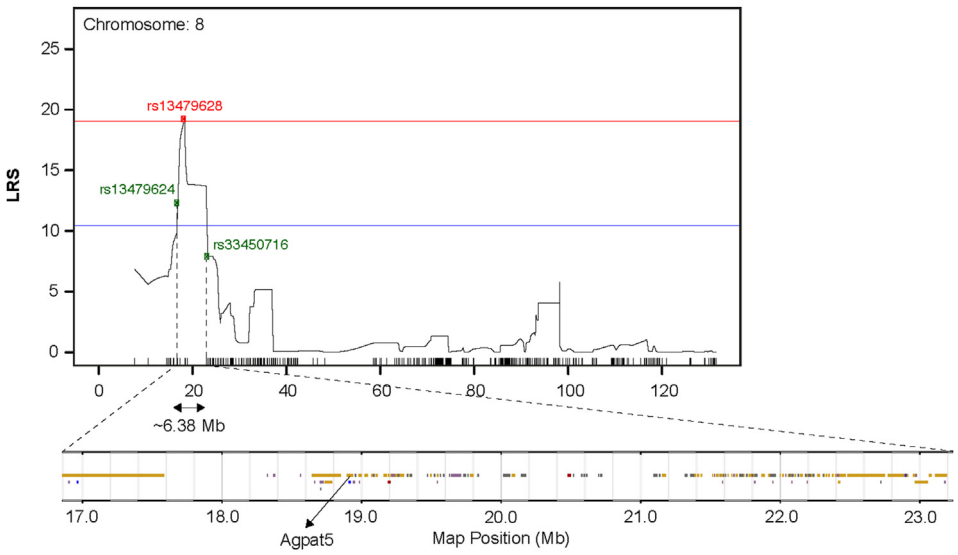

B

Rank	Gene	r	p value	TPM
1	2610005L07Rik	-0.5768	0.0002	30.37
2	Agpat5	0.4940	0.0016	60.86
3	LOC547150	0.4509	0.0045	31.95

Figure 2: Candidate genes in chromosome 8 QTL. A: Localization of the QTL on chromosome 8 between markers rs13479624 and rs33450716 with a peak LRS = 19.23 on marker rs13479628. The QTL spans ~6.38 Mb and contains 155 genes. B: Table showing chromosome 8 QTL genes with hypothalamic expression correlated to insulin-induced glucagon secretion ranked by p-value. r: Pearson's correlation coefficient. TPM: mean hypothalamic expression among BXD strains in transcripts per million.

mice previously injected with saline or Anakinra (Figure 5C). In DBA/2J mice, i.c.v. Anakinra had no effect on glycemia after i.p. saline (Figure 5D) but led to a deeper hypoglycemia after insulin injection (Figure 5E) and a markedly increased insulin-induced glucagon secretion (Figure 5F). Thus, increased insulin-induced glucagon secretion following the inhibition of Il-1β signaling in DBA/2J mice could result from increased insulin sensitivity, thereby causing more severe hypoglycemia and/or to higher sensitivity to hypoglycemia of the glucose-sensing system controlling glucagon secretion.

To determine whether hypoglycemia sensing in DBA/2J mice was affected by Il-1β signaling, we performed hyperinsulinemic-hypoglycemic clamps in mice injected i.c.v. with saline or Anakinra. Insulin was infused at a constant rate and glucose at a variable rate to reach ~2.5 mM (Figure 5G). Anakinra administration did not affect the glucose infusion rate (Figure 5H) but significantly increased glucagon secretion (Figure 5I). Thus, in DBA/2J mice, Il-1β signaling negatively controlled hypoglycemia sensing and glucagon secretion.

3.3. Il-1β antagonism increases hypoglycemia-activated autonomic nervous activity in DBA/2J mice

To determine whether ARH and PVN were also sensitive to hypoglycemia in DBA/2J mice and whether Anakinra would increase this sensitivity, we injected mice with i.c.v. saline or i.c.v. Anakinra and 1 h later with i.p. insulin and prepared their brains 2 h later for c-fos immunofluorescence microscopy detection. One hour after insulin injection, the two groups of mice reached the same glycemic level (3.48 ± 0.32 mM vs. 3.91 ± 0.37 mM after saline and Anakinra administration, respectively). In the ARH (Figure 6A–E) and PVN (Figure 6F–J), we found that Anakinra administration significantly increased insulin-induced neuronal activation as compared to saline treatment.

The ARH and PVN nuclei are connected to pre-autonomic neurons [42–45] that control both the parasympathetic (PNS) and sympathetic (SNS) nerves, which when activated by hypoglycemia trigger glucagon secretion [46]. Thus, we next recorded PNS and SNS activities in DBA/2J mice that received either i.c.v. saline or Anakinra before i.p. insulin. Upon insulin-induced hypoglycemia, we observed no increase in PNS activity in DBA/2J mice pre-injected with saline. This activity was, however, markedly higher following i.c.v. Anakinra injection (Figure 7AandB). Similarly, while insulin did not induce SNS activity in mice pre-injected with saline, a marked activation was observed in mice pre-injected with Anakinra (Figure 7C and D).

3.4. Copine 8 and insulin-induced glucagon secretion

As shown in Figure 3B, *Tmem117* was the second-best correlated gene with the glucagon trait; its characterization and role in controlling glucagon secretion will be the subject of another publication. The next genes in the list were *Pdzrn4*, a PDZ domain and ring domain containing protein that may be involved in the control of cell proliferation; *Prickle1*, a nuclear hormone receptor and possible regulator of the Wnt/beta-catenin signaling pathway; *Gxylt1*, encoding a glucoside xylosetransferase; *Zcrb1*, a zinc finger containing RNA binding protein involved in splicing; *Cpne8*, a Ca^{++}-dependent and CII domain-containing protein, and *Twf1*, an actin-binding protein.

Copine8 is involved in Ca^{++}-dependent regulation of membrane trafficking and exocytosis [47] and, thus, synaptic vesicle release upon membrane depolarization. In addition, we found that the expression of the *Cpne8* mRNA was enriched in the VMN (Fig. S1A), and its

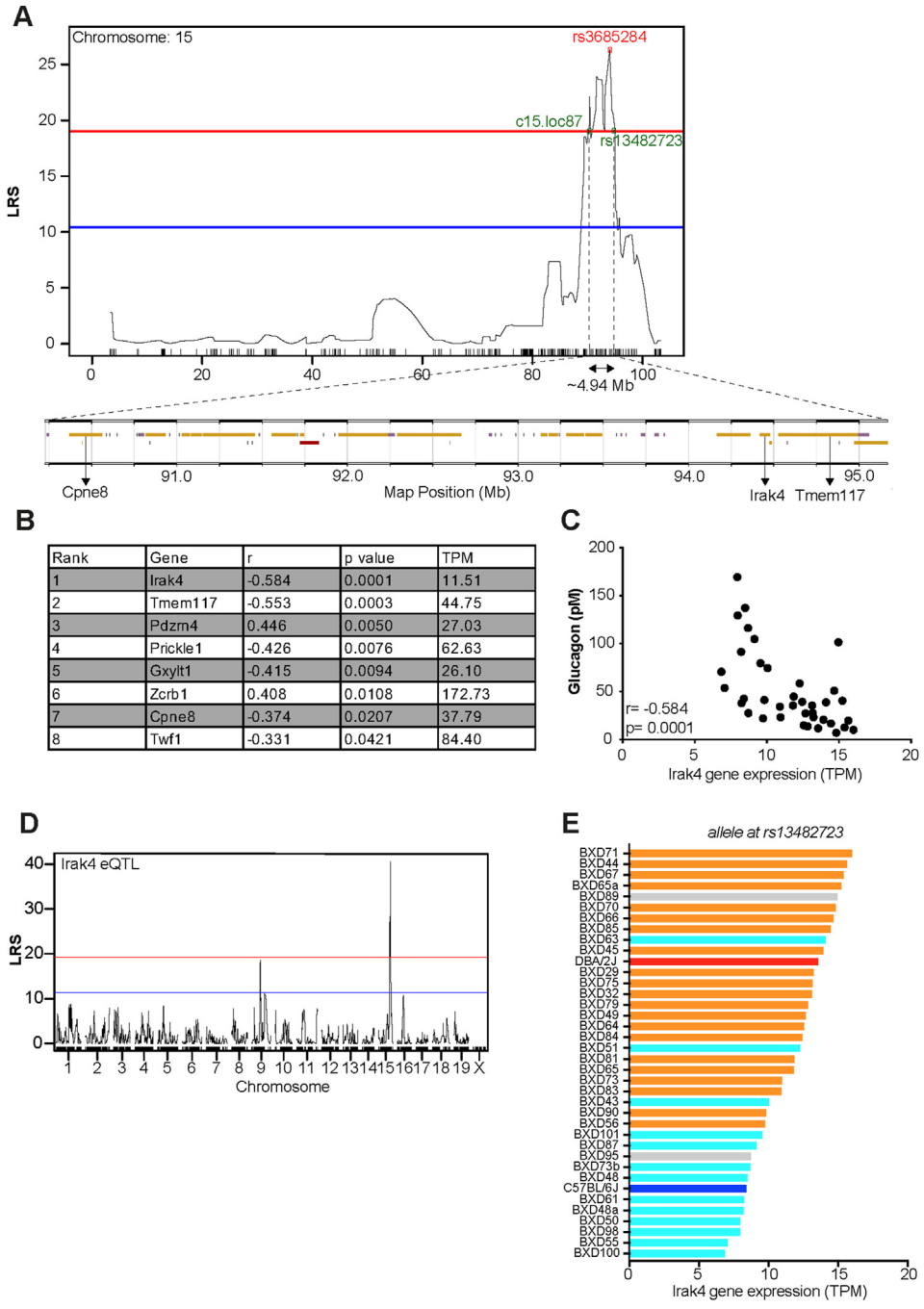

Rank	Gene	r	p value	TPM
1	Irak4	-0.584	0.0001	11.51
2	Tmem117	-0.553	0.0003	44.75
3	Pdzrn4	0.446	0.0050	27.03
4	Prickle1	-0.426	0.0076	62.63
5	Gxylt1	-0.415	0.0094	26.10
6	Zcrb1	0.408	0.0108	172.73
7	Cpne8	-0.374	0.0207	37.79
8	Twf1	-0.331	0.0421	84.40

Figure 3: Candidate genes in chromosome 15 QTL. A: Localization of the QTL on chromosome 15 between markers c15.loc87 and rs13482723 with a peak LRS = 26.27 on marker rs3685284. The QTL spans ~4.94 Mb and contains 42 genes. **B**: Table showing the chromosome 15 QTL genes with hypothalamic expression correlated to insulin-induced glucagon secretion ranked by p-value. r: Pearson's correlation coefficient. TPM: mean hypothalamic expression among BXD strains in transcripts per million. **C**: Scatterplot of the correlation between plasma glucagon and hypothalamic *Irak4* expression in BXD mice and their parental strains. **D**: eQTL mapping identifies a cis eQTL on chromosome 15 controlling *Irak4* expression between markers rs3685284 and rs45781537 with peak LRS = 40.6 at rs13482723. **E**: Effect of DBA/2J and C57BL/6J alleles at rs13482723 on hypothalamic *Irak4* expression. Orange: BXD strains with DBA/2J allele; Cyan: BXD strains with C57BL/6J allele; Gray: heterozygous mice; Red: DBA/2J mice; Blue: C57BL/6J mice.

hypothalamic expression was under the control of a cis eQTL located in the QTL of chromosome 15, between markers rs13482702 and rs45781537 with peak LRS = 22.9 (Fig. S1B). Thus, to explore the potential role of *Cpne8* in insulin-induced glucagon secretion, we generated mice with whole body *Cpne8* inactivation (Fig. S1C). Recombination of the gene was confirmed by PCR analysis (Fig. S1D), and quantitative RT-PCR demonstrated a complete loss of *Cpne8* expression in the hypothalamus of $Cpne8^{-/-}$ mice as compared to that in $Cpne8^{+/+}$ mice (Fig. S1E). Saline- and insulin-induced glucagon secretion were assessed as described above. We found that *Cpne8*

Table 1 — Differential expression of genes belonging to the Il-1R and TlR signaling pathways in the hypothalamus of DBA/2J vs. C57BL/6J mice.

Pathway	Gene list	Differential gene expression in the hypothalamus of DBA/2J vs. C57BL/6J mice (LogFC)
Il-1r signaling	Il-1a	−0.282
	Il-1b	2.524
	Il-1r1	−0.566
	Il-1r2	−0.368
	Il-1rap	−0.228
Tlr signaling	Tlr1	−0.382
	Tlr2	−0.169
	Tlr3	−0.116
	Tlr4	0.046
	Tlr5	−0.810
	Tlr6	1.399
	Tlr7	0.075
	Tlr9	−0.848
	Tlr12	−0.760
	Tlr13	0.405
Common signaling	Myd88	−0.527
	Irak4	0.689

inactivation had no impact on insulin-induced hypoglycemia (Fig. S1F) and insulin-induced glucagon secretion (Figure 1G).

4. DISCUSSION

The present genetic and genomic screenings identified two QTLs involved in the control of hypoglycemia-induced glucagon secretion. In the QTL of chromosome 8, three genes showed expression levels strongly correlated with the glucagon secretion trait, named *Agpat5* and two genes encoding proteins of unknown function. In the QTL of chromosome 15, 8 genes showed significant correlations with the glucagon trait. Here, we focused on the role of hypothalamic *Irak4* and *Cpne8*. We found that in DBA/2J mice, which display a very low glucagon response to insulin-induced hypoglycemia, the level of hypothalamic *Irak4* and of *Il-1ß* were significantly higher than that in the hypothalamus of C57BL/6J mice. We found that blocking hypothalamic Il-1R signaling in DBA/2J mice markedly increased hypoglycemia-induced glucagon secretion, c-fos expression in the ARH and PVN, and parasympathetic and sympathetic nerve activities. Collectively, our data suggest that hypothalamic *Irak4* expression is genetically determined and that elevated *Irak4* expression limits hypoglycemia-induced glucagon secretion.

In a previous genetic screening for genes controlling glucagon secretion induced by 2DG-induced neuroglucopenia, a procedure often used as a substitute for insulin-induced hypoglycemia, we identified a QTL on chromosome 7 and *Fgf15* as a candidate gene. We found that *Fgf15* expression defines a subpopulation of neurons in the DMH which, when activated suppress PNS activity and glucagon secretion but stimulate SNS activity to increase hepatic glucose production [30,31]. Our present screening for insulin-induced glucagon secretion identified two different QTLs on chromosomes 8 and 15. Thus, the central mechanisms of neuroglucopenia- and hypoglycemia-induced glucagon secretion recruit different neuronal circuits. This is not too surprising as 2DG suppresses glycolysis and ATP production, which leads to a rapid CRR and a marked hyperglycemia, whereas insulin can affect neuronal activity by binding to neuronal insulin receptors and/or as a result of the slowly developing hypoglycemia. Thus, our genetic data confirm that 2DG recruits non-overlapping neuronal circuits, both of which, however, converge on pre-autonomic regions to control PNS and SNS activity. This further supports the notion that hypoglycemia detection by the brain consists of a distributed glucose-sensing system, which is precisely integrated to control the counterregulatory response.

Irak4 encodes a protein kinase acting downstream of the Il-1R and TlRs [32,38,48]. Upon ligand binding, the Il-1R heterodimerizes with the Il-1R accessory protein (IL-Rap), and TlRs homodimerize or heterodimerize with other TlRs. These dimers associate *via* their

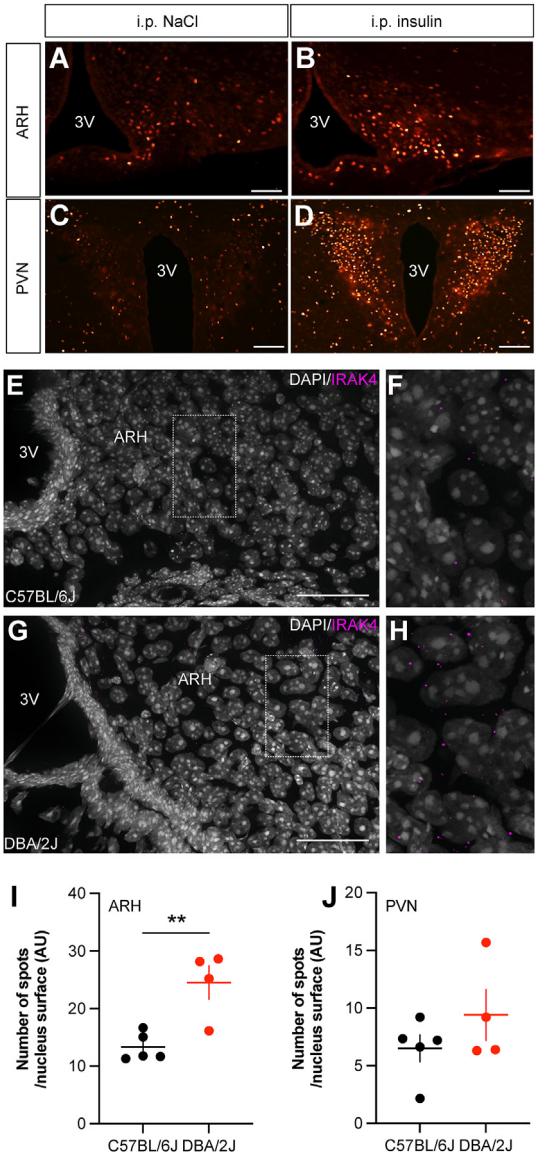

Figure 4: Hypoglycemia-induced neuronal activation and *Irak4* expression in the hypothalamus of C57BL/6J and DBA/2J mice. A-B: Representative micrographs of c-fos-positive cells in the ARH 2 h after i.p. NaCl (**A**) or insulin injection (**B**) in C57BL/6J mice. Scale bar = 100 µm. **C-D**: Representative micrographs of c-fos-positive cells in the PVN 2 h after i.p. NaCl (**C**) or insulin injection (**D**) in C57BL/6J mice. Scale bar = 100 µm. **E-F**: Representative micrographs of *Irak4* expression in the ARH of C57BL/6J mice. Scale bar: 50 µm. **G-H**: Representative micrographs of *Irak4* expression in the ARH of C57BL/6J mice. Scale bar: 50 µm. **I**: Number of *Irak4* mRNA spots in the ARH of the hypothalamus of C57BL/6J as compared to that in DBA/2J mice. (n = 5 and 4 mice; total number of spots counted: 845 and 1403 for C57BL/6J and. DBA/2J mice, respectively). **J**: Number of *Irak4* mRNA spots in the PVN of C57BL/6J as compared to that in BA/2J mice. (n = 5 and 4 mice; total number of spots counted: 433 and 338 for C57BL/6J and. DBA/2J mice, respectively). Data are expressed as means ± SEM. **p < 0.005. Student's t-test (**I**).

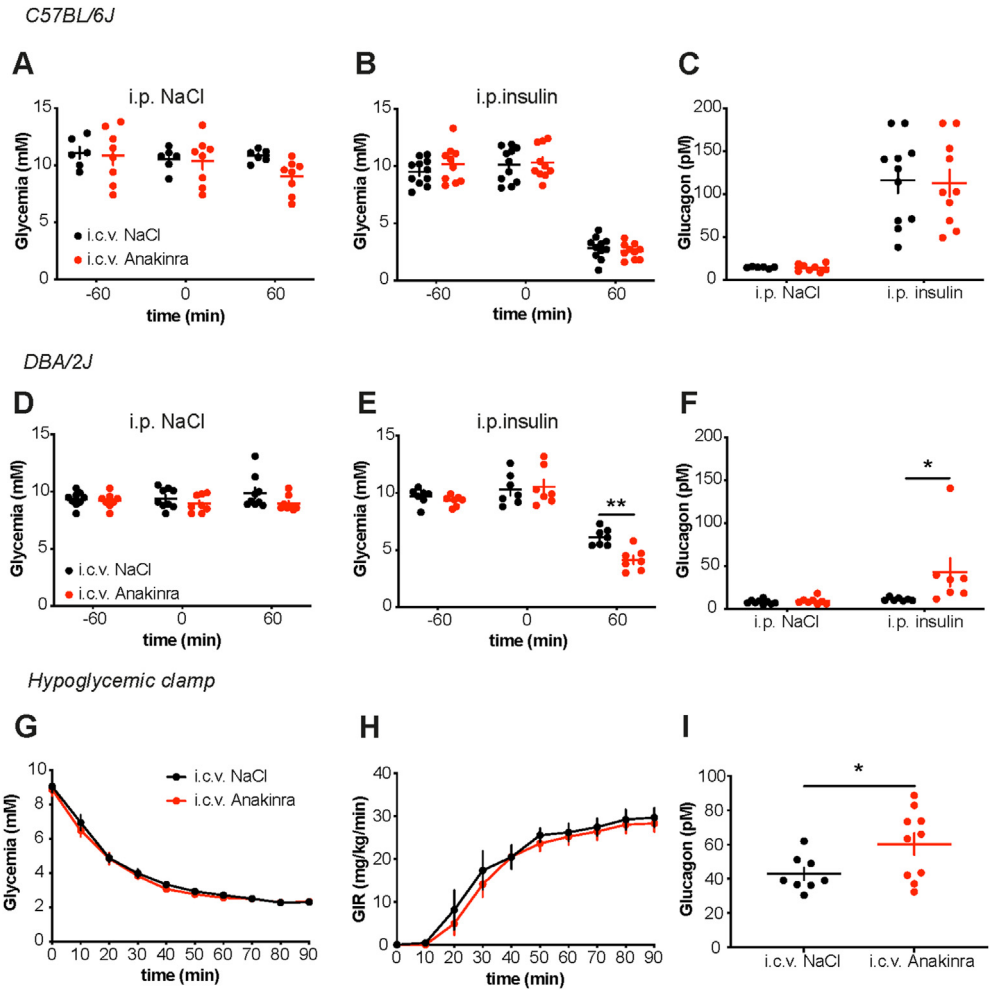

Figure 5: Inhibition of Il-1R signaling restores hypoglycemia-induced glucagon secretion in DBA/2J mice. A: Glycemia in C57BL/6J mice injected i.c.v. with NaCl 0.9% or Anakinra at −60 min and i.p. with NaCl 0.9% at 0 min (n = 6–8). **B**: Glycemia in C567BL/6J mice injected i.c.v. with NaCl 0.9% or Anakinra at −60 min and i.p. with Anakinra at 0 min (n = 10–11). **C**: Plasma glucagon 60 min after i.p. injection of NaCl 0.9% or insulin in C57BL/6J mice that received i.c.v. injection of NaCl 0.9% or Anakinra at −60 min (n = 6–11). **D**: Glycemia in DBA/2J mice injected i.c.v. with NaCl 0.9% or Anakinra at −60 min and i.p. with NaCl 0.9% at 0 min (n = 7–9). **E**: Glycemia in DBA/2J mice injected i.c.v. with NaCl 0.9% or Anakinra at −60 min and i.p. with Anakinra at 0 min (n = 7). **F**: Plasma glucagon 60 min after i.p. injection of NaCl 0.9% or insulin in DBA/2J mice that received i.c.v. injection of NaCl 0.9% or Anakinra at −60 min (n = 7–9). **G-I**: Hyperinsulinemic-hypoglycemic clamps in DBA/2J mice that received i.c.v. NaCl or Anakinra at 0 min. **I**: Plasma glucagon measured at 90 min (n = 8–10). Data are means ± SEM. *p < 0.05; **p < 0.005. Mixed effects analysis followed by Sidak's multiple comparisons test (E and F). Student's t-test (I).

cytoplasmic Toll/interleukin-1 receptor domains to the adaptor protein Myd88, which recruits Irak4 to induce the synthesis of pro-inflammatory cytokines such as Il-1β, Il-6 and TNFα through the NF-κB and MAPK signaling pathways [49,50]. The role of *Irak4* in the response to TIR ligands and innate immunity is well characterized [38]. Its role in glucoregulation or specifically in the CRR is less well established.

Irak4 is expressed at a higher level in the hypothalamus of DBA/2J mice as compared to that in C57BL/6J mice, and *in situ* hybridization experiments showed that *Irak4* is widely distributed in the hypothalamus of both strains with a markedly higher expression in the ARH, but not in the PVN, of DBA2/J mice, suggesting that the ARH is where *Irak4* has a major role in controlling the differential glucagon response to hypoglycemia. The expression of *Il-1ß* was also found to be higher in the hypothalamus of DBA/2J mice. As our genetic screening identified *Irak4*, not *Il-1ß* as a genetic determinant of glucagon secretion, this suggests that *Irak4* is at the center of an autoregulated signaling loop that controls *Il-1ß* expression, Il-1R signaling and, eventually glucagon secretion. To determine whether the high expression of *Irak4* and Il-1R signaling was the cause of the lower glucagon secretion in DBA/2J mice, we blocked Il-1R signaling by i.c.v. injection of Anakinra before insulin-induced hypoglycemia. This increased glucagon secretion in DBA/2J mice but not in C57BL/6J mice. In DBA/2J mice, this was associated with an increased expression of c-fos in the ARH and the PVN, and with enhanced PNS and SNS nervous activity upon insulin-induced hypoglycemia. It is well known that ARH and PVN neurons can regulate PNS activity through their projections to the DVC [51] and AgRP neurons of the ARH, 40% of which are GI neurons [52] that innervate neurons of the PVN, which regulate SNS outflow to the liver, the pancreas, and the adrenal medulla [53–55].

In hyperinsulinemic-hypoglycemic clamps we also found that pre-treatment with Anakinra increased glucagon secretion at the end of the hypoglycemic period. This experiment confirmed that Il-1R signaling modulates hypoglycemia-induced glucagon secretion in DBA/2J mice.

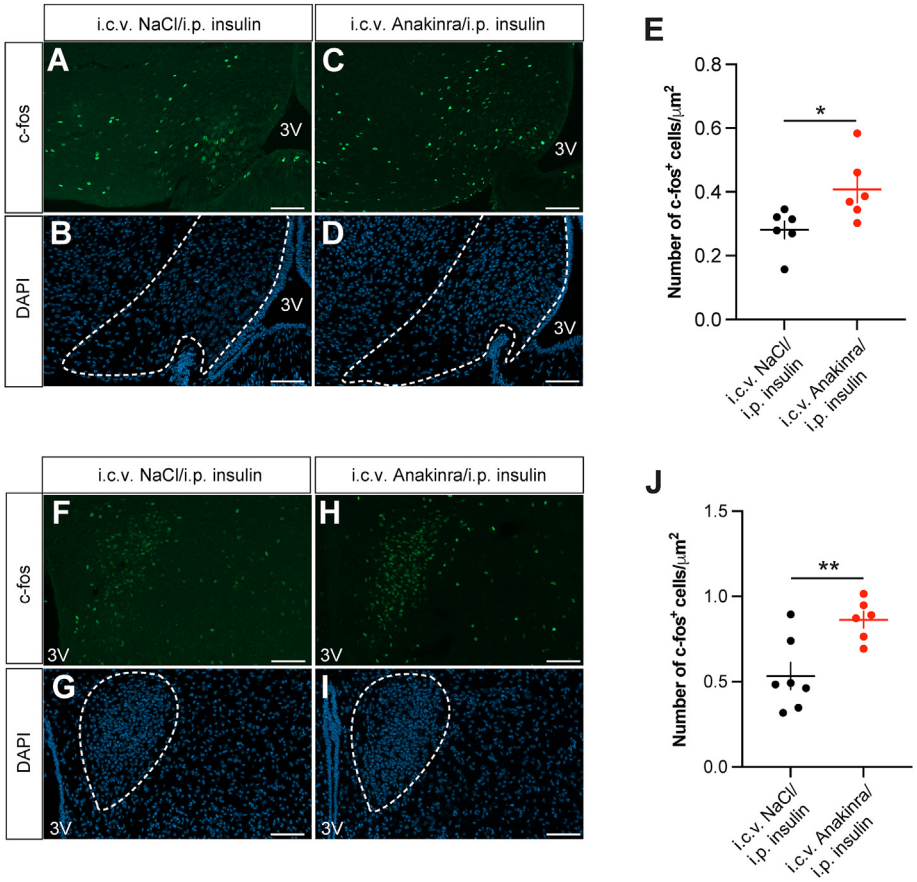

Figure 6: Inhibition of Il-1R signaling restores hypoglycemia-induced neuronal activation in DBA/2J mice. **A-D**: DBA/2J mice received i.c.v. NaCl or Anakinra. One hour later, they received i.p. insulin and were killed 2 h later. Representative micrographs of the ARH showing c-fos staining (**A,C**) or DAPI staining (**B,D**). Scale bar = 50 μm. **E:** Quantification of c-fos-positive cells in the ARH. **F—I**: The same DBA/2J mice as shown in **A-D**. Representative micrographs of the PVN showing c-fos staining (**F,H**) and DAPI staining (**G,I**). Scale bar = 50 μm. **J**: Quantification of c-fos positive cells in the PVN. Data are means ± SEM. *p < 0.05; **p < 0.005. Student's t-test (E and J).

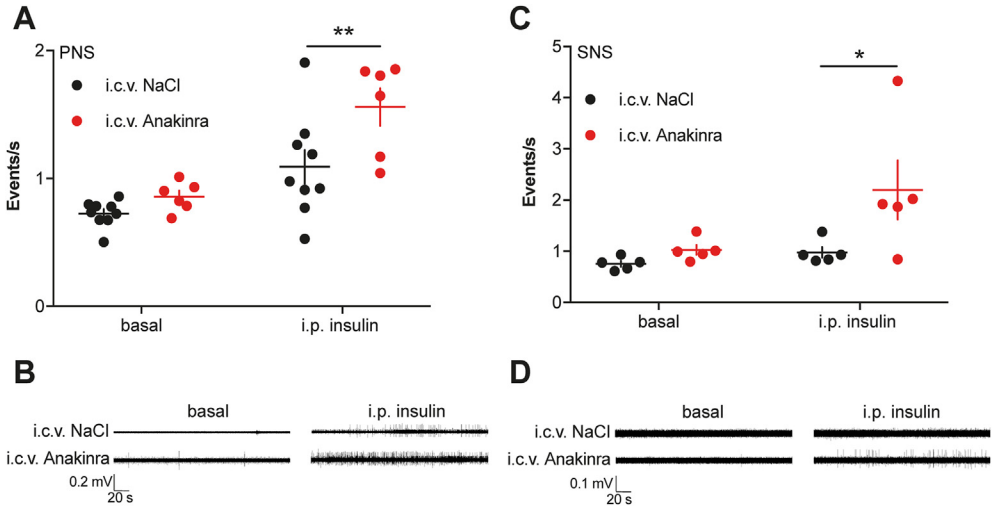

Figure 7: Inhibition of Il-1R signaling restored hypoglycemia-induced autonomous nervous activity in DBA/2J mice. **A-B**: Parasympathetic nerve firing in the basal state or following i.p. insulin injection in DBA/2J mice that received i.c.v. injections of NaCl 0.9% or Anakinra 60 min before starting the recording. **A**: quantification of the firing activity and **B**: representative trace (n = 5 to 9). **C-D**: Sympathetic nerve firing in the basal state or following i.p. insulin injection in DBA/2J mice that received i.c.v. injections of NaCl 0.9% or Anakinra 60 min before starting the recording. **C**: quantification of the firing activity and **D**: representative trace (n = 5). Data are expressed as means ± SEM. *p < 0.05; **p < 0.005. Repeated-measures two-way ANOVA followed by Sidak's multiple comparisons test (A and C).

This was an important point to verify as Anakinra pre-treatment of DBA/2J mice also led to deeper insulin-induced hypoglycemia than in saline pre-injected mice, suggesting that hypothalamic Il-1R signaling may also control insulin sensitivity. This aspect of Il-1β action will require further investigations.

Il-1β is expressed widely in the brain, neurons, astrocytes, and microglial cells [56,57]. Its expression can be induced by hypoglycemia, which induces an inflammatory reaction in the brain [57—59]. Previous studies have shown that i.p. injections of Il-1β induce hypoglycemia, associated with augmented insulin secretion [60,61], increased glucose utilization, and reduced hepatic glucose production [62]. Intraperitoneal injection of Il-1β also stimulates *Il-1β* mRNA expression in the hypothalamus, and the associated hypoglycemia is markedly reduced by i.c.v. injection of an Il-1R antagonist [63], indicating that the central Il-1β signaling pathway negatively impacts the CRR. The role of hypothalamic Il-1β in suppressing the counterregulatory response is further supported by a recent observation that hypoglycemia-activated microglial cells release cytokines, including Il-1β, in close proximity to NPY/AgRP neurons leading to impaired CRR [57]. In this context, our study shows that hypothalamic Il-1β signaling is a physiological regulator of glucagon secretion and the CRR.

Il-1β-induced hypoglycemia, in contrast to that induced by insulin, does not stimulate food consumption [64], a response that involves the activation of AgRP neurons [65]. A possible explanation for a lack of feeding stimulation is that Il-1β increases glucose utilization by neurons and astrocytes [66,67]. Thus, even though hypoglycemia develops, the metabolic effect of Il-1β may prevent cellular energy depletion and the consequent activation of AMP-dependent protein kinase, which is required for the activation of GI neurons [23,68]. Therefore, prolonged inflammatory conditions, such as those induced by multiple hypoglycemic episodes, which increase central Il-1β production may contribute to HAAF.

In summary, our genetic and transcriptomic screening identified novel candidate genes controlling the physiological response of the brain to hypoglycemia. We showed that the hypothalamic Il-1R/Irak4 signaling pathway, through a genetic control of *Irak4* expression, is differentially expressed depending on the mouse genetic background, and an increased activity of this pathway negatively impacts insulin-induced glucagon secretion. This likely depends on the known effect of Il-1β to increase neuronal and astrocyte glucose metabolism, thereby preventing the normal activation of GI neurons by hypoglycemia. In DBA/2J mice, blocking Il-1R signaling increased the response of ARH and PVN neurons to hypoglycemia, the activation of both branches of the autonomic nervous system, and the secretion of glucagon. Collectively, our results provide new genetic and cellular information about the complexity of central hypoglycemia sensing and the counterregulatory response. They will also pave the way for a better understanding of how insulin induces hypoglycemia associated autonomic failure in diabetic patients.

ACKNOWLEDGMENTS

This work was supported by a European Research Council Advanced Grant (INTEGRATE, No. 694798) and a Swiss National Science Foundation grant (310030—182496) to BT and has received funding from the Innovative Medicines Initiative 2 Joint Undertaking (JU) under grant agreement No 777460 (HypoRESOLVE). The JU receives support from the European Union's Horizon 2020 research and innovation programme and EFPIA and T1D Exchange, JDRF, International Diabetes Federation (IDF), and The Leona M. and Harry B. Helmsley Charitable Trust.

CONFLICT OF INTEREST

The authors report no conflict of interest. JCA is an employee of Novo Nordisk.

APPENDIX A. SUPPLEMENTARY DATA

Supplementary data to this article can be found online at https://doi.org/10.1016/j.molmet.2022.101479.

AUTHOR CONTRIBUTIONS

BT and AP conceived the project and designed the experiments. AP, XB, JCA, DT, and SC performed the experiments. AP, MJ, and ARSA analyzed the genetic and transcriptomic data. AP, JCA, and BT analyzed the data and wrote the paper.

REFERENCES

[1] Unger, R.H., Orci, L., 1981. Glucagon and the A cell: physiology and pathophysiology (first two parts). New England Journal of Medicine 304(25):1518—1524.

[2] Donovan, C.M., Watts, A.G., 2014. Peripheral and central glucose sensing in hypoglycemic detection. Physiology (Bethesda) 29(5):314—324.

[3] Jackson, P.A., Cardin, S., Coffey, C.S., Neal, D.W., Allen, E.J., Penaloza, A.R., et al., 2000. Effect of hepatic denervation on the counterregulatory response to insulin-induced hypoglycemia in the dog. American Journal of Physiology. Endocrinology and Metabolism 279(6):E1249—E1257.

[4] Verberne, A.J., Sabetghadam, A., Korim, W.S., 2014. Neural pathways that control the glucose counterregulatory response. Frontiers in Neuroscience 8:38.

[5] Cryer, P.E., 2013. Mechanisms of hypoglycemia-associated autonomic failure in diabetes. New England Journal of Medicine 369(4):362—372.

[6] Stanley, S., Moheet, A., Seaquist, E.R., 2019. Central mechanisms of glucose sensing and counterregulation in defense of hypoglycemia. Endocrine Reviews 40(3):768—788.

[7] Steinbusch, L., Labouebe, G., Thorens, B., 2015. Brain glucose sensing in homeostatic and hedonic regulation. Trends in Endocrinology and Metabolism 26(9):455—466.

[8] Routh, V.H., 2002. Glucose-sensing neurons: are they physiologically relevant? Physiology & Behavior 76(3):403—413.

[9] Thorens, B., 2011. Brain glucose sensing and neural regulation of insulin and glucagon secretion. Diabetes, Obesity and Metabolism 13(Suppl 1):82—88.

[10] Flak, J.N., Patterson, C.M., Garfield, A.S., D'Agostino, G., Goforth, P.B., Sutton, A.K., et al., 2014. Leptin-inhibited PBN neurons enhance responses to hypoglycemia in negative energy balance. Nature Neuroscience 17(12):1744—1750.

[11] Garfield, A.S., Shah, B.P., Madara, J.C., Burke, L.K., Patterson, C.M., Flak, J., et al., 2014. A parabrachial-hypothalamic cholecystokinin neurocircuit controls counterregulatory responses to hypoglycemia. Cell Metabolism 20(6):1030—1037.

[12] Meek, T.H., Nelson, J.T., Matsen, M.E., Dorfman, M.D., Guyenet, S.J., Damian, V., et al., 2016. Functional identification of a neurocircuit regulating blood glucose. Proceedings of the National Academy of Sciences of the United States of America 113(14):E2073—E2082.

[13] Tong, Q., Ye, C., McCrimmon, R.J., Dhillon, H., Choi, B., Kramer, M.D., et al., 2007. Synaptic glutamate release by ventromedial hypothalamic neurons is part of the neurocircuitry that prevents hypoglycemia. Cell Metabolism 5(5):383—393.

[14] Marty, N., Dallaporta, M., Thorens, B., 2007. Brain glucose sensing, counterregulation, and energy homeostasis. Physiology (Bethesda) 22:241—251.

[15] Levin, B.E., Becker, T.C., Eiki, J., Zhang, B.B., Dunn-Meynell, A.A., 2008. Ventromedial hypothalamic glucokinase is an important mediator of the

counterregulatory response to insulin-induced hypoglycemia. Diabetes 57(5): 1371–1379.
[16] Stanley, S., Domingos, A.I., Kelly, L., Garfield, A., Damanpour, S., Heisler, L., et al., 2013. Profiling of glucose-sensing neurons reveals that GHRH neurons are activated by hypoglycemia. Cell Metabolism 18(4):596–607.
[17] Ashford, M.L., Boden, P.R., Treherne, J.M., 1990. Tolbutamide excites rat glucoreceptive ventromedial hypothalamic neurones by indirect inhibition of ATP-K+ channels. British Journal of Pharmacology 101(3):531–540.
[18] Miki, T., Liss, B., Minami, K., Shiuchi, T., Saraya, A., Kashima, Y., et al., 2001. ATP-sensitive K+ channels in the hypothalamus are essential for the maintenance of glucose homeostasis. Nature Neuroscience 4(5):507–512.
[19] Steinbusch, L.K., Picard, A., Bonnet, M.S., Basco, D., Labouebe, G., Thorens, B., 2016. Sex-specific control of fat mass and counterregulation by hypothalamic glucokinase. Diabetes 65(10):2920–2931.
[20] O'Malley, D., Reimann, F., Simpson, A.K., Gribble, F.M., 2006. Sodium-coupled glucose cotransporters contribute to hypothalamic glucose sensing. Diabetes 55(12):3381–3386.
[21] Alquier, T., Kawashima, J., Tsuji, Y., Kahn, B.B., 2007. Role of hypothalamic adenosine 5'-monophosphate-activated protein kinase in the impaired counterregulatory response induced by repetitive neuroglucopenia. Endocrinology 148(3):1367–1375.
[22] McCrimmon, R.J., Shaw, M., Fan, X., Cheng, H., Ding, Y., Vella, M.C., et al., 2008. Key role for AMP-activated protein kinase in the ventromedial hypothalamus in regulating counterregulatory hormone responses to acute hypoglycemia. Diabetes 57(2):444–450.
[23] Quenneville, S., Labouèbe, G., Basco, D., Metref, S., Viollet, B., Foretz, M., et al., 2020. Hypoglycemia-sensing neurons of the ventromedial hypothalamus require AMPK-induced Txn2 expression but are dispensable for physiological counterregulation. Diabetes 69(11):2253–2266.
[24] Murphy, B.A., Fakira, K.A., Song, Z., Beuve, A., Routh, V.H., 2009. AMP-activated protein kinase and nitric oxide regulate the glucose sensitivity of ventromedial hypothalamic glucose-inhibited neurons. American Journal of Physiology - Cell Physiology 297(3):C750–C758.
[25] He, Y., Xu, P., Wang, C., Xia, Y., Yu, M., Yang, Y., et al., 2020. Estrogen receptor-alpha expressing neurons in the ventrolateral VMH regulate glucose balance. Nature Communications 11(1):2165.
[26] Lamy, C.M., Sanno, H., Labouebe, G., Picard, A., Magnan, C., Chatton, J.Y., et al., 2014. Hypoglycemia-activated GLUT2 neurons of the nucleus tractus solitarius stimulate vagal activity and glucagon secretion. Cell Metabolism 19(3):527–538.
[27] Kurita, H., Xu, K.Y., Maejima, Y., Nakata, M., Dezaki, K., Santoso, P., et al., 2015. Arcuate Na+,K+-ATPase senses systemic energy states and regulates feeding behavior through glucose-inhibited neurons. American Journal of Physiology. Endocrinology and Metabolism 309(4):E320–E333.
[28] Silver, I.A., Erecinska, M., 1998. Glucose-induced intracellular ion changes in sugar-sensitive hypothalamic neurons. Journal of Neurophysiology 79(4): 1733–1745.
[29] Peirce, J.L., Lu, L., Gu, J., Silver, L.M., Williams, R.W., 2004. A new set of BXD recombinant inbred lines from advanced intercross populations in mice. BMC Genetics 5:7.
[30] Picard, A., Metref, S., Tarussio, D., Dolci, W., Berney, X., Croizier, S., et al., 2021. Fgf15 neurons of the dorsomedial hypothalamus control glucagon secretion and hepatic gluconeogenesis. Diabetes.
[31] Picard, A., Soyer, J., Berney, X., Tarussio, D., Quenneville, S., Jan, M., et al., 2016. A genetic screen identifies hypothalamic Fgf15 as a regulator of glucagon secretion. Cell Reports 17(7):1795–1806.
[32] Li, S., Strelow, A., Fontana, E.J., Wesche, H., 2002. IRAK-4: a novel member of the IRAK family with the properties of an IRAK-kinase. Proceedings of the National Academy of Sciences of the United States of America 99(8):5567–5572.
[33] Berdous, D., Berney, X., Sanchez-Archidona, A.R., Jan, M., Roujeau, C., Lopez-Mejia, I.C., et al., 2020. A genetic screen identifies Crat as a regulator of pancreatic beta-cell insulin secretion. Molecular Metabolism 37:100993.
[34] Broman, K., Sen, S., 2009. A Guide to QTL mapping with R/qtl.
[35] Paxinos, G., watson, C., 1982. The rat brain in stereotaxic coordinates.
[36] Burcelin, R., Thorens, B., 2001. Evidence that extrapancreatic GLUT2-dependent glucose sensors control glucagon secretion. Diabetes 50(6): 1282–1289.
[37] Maitra, R., Grigoryev, D.N., Bera, T.K., Pastan, I.H., Lee, B., 2003. Cloning, molecular characterization, and expression analysis of Copine 8. Biochemical and Biophysical Research Communications 303(3):842–847.
[38] Suzuki, N., Suzuki, S., Duncan, G.S., Millar, D.G., Wada, T., Mirtsos, C., et al., 2002. Severe impairment of interleukin-1 and Toll-like receptor signalling in mice lacking IRAK-4. Nature 416(6882):750–756.
[39] Diessler, S., Jan, M., Emmenegger, Y., Guex, N., Middleton, B., Skene, D.J., et al., 2018. A systems genetics resource and analysis of sleep regulation in the mouse. PLoS Biology 16(8):e2005750.
[40] Keane, T.M., Goodstadt, L., Danecek, P., White, M.A., Wong, K., Yalcin, B., et al., 2011. Mouse genomic variation and its effect on phenotypes and gene regulation. Nature 477(7364):289–294.
[41] McLaren, W., Gil, L., Hunt, S.E., Riat, H.S., Ritchie, G.R., Thormann, A., et al., 2016. The ensembl variant effect predictor. Genome Biology 17(1):122.
[42] Bouyer, K., Simerly, R.B., 2013. Neonatal leptin exposure specifies innervation of presympathetic hypothalamic neurons and improves the metabolic status of leptin-deficient mice. Journal of Neuroscience 33(2):840–851.
[43] Elias, C.F., Lee, C., Kelly, J., Aschkenasi, C., Ahima, R.S., Couceyro, P.R., et al., 1998. Leptin activates hypothalamic CART neurons projecting to the spinal cord. Neuron 21(6):1375–1385.
[44] Shah, B.P., Vong, L., Olson, D.P., Koda, S., Krashes, M.J., Ye, C., et al., 2014. MC4R-expressing glutamatergic neurons in the paraventricular hypothalamus regulate feeding and are synaptically connected to the parabrachial nucleus. Proceedings of the National Academy of Sciences of the United States of America 111(36):13193–13198.
[45] Swanson, L.W., Sawchenko, P.E., 1980. Paraventricular nucleus: a site for the integration of neuroendocrine and autonomic mechanisms. Neuroendocrinology 31(6):410–417.
[46] Taborsky Jr., G.J., Mundinger, T.O., 2012. Minireview: the role of the autonomic nervous system in mediating the glucagon response to hypoglycemia. Endocrinology 153(3):1055–1062.
[47] Creutz, C.E., Tomsig, J.L., Snyder, S.L., Gautier, M.C., Skouri, F., Beisson, J., et al., 1998. The copines, a novel class of C2 domain-containing, calcium-dependent, phospholipid-binding proteins conserved from Paramecium to humans. Journal of Biological Chemistry 273(3):1393–1402.
[48] Suzuki, N., Saito, T., 2006. IRAK-4–a shared NF-kappaB activator in innate and acquired immunity. Trends in Immunology 27(12):566–572.
[49] Ferrao, R., Li, J., Bergamin, E., Wu, H., 2012. Structural insights into the assembly of large oligomeric signalosomes in the Toll-like receptor-interleukin-1 receptor superfamily. Science Signaling 5(226):re3.
[50] Verstrepen, L., Bekaert, T., Chau, T.L., Tavernier, J., Chariot, A., Beyaert, R., 2008. TLR-4, IL-1R and TNF-R signaling to NF-kappaB: variations on a common theme. Cellular and Molecular Life Sciences 65(19):2964–2978.
[51] Holt, M.K., Pomeranz, L.E., Beier, K.T., Reimann, F., Gribble, F.M., Rinaman, L., 2019. Synaptic inputs to the mouse dorsal vagal complex and its resident preproglucagon neurons. Journal of Neuroscience 39(49):9767–9781.
[52] Fioramonti, X., Contie, S., Song, Z., Routh, V.H., Lorsignol, A., Penicaud, L., 2007. Characterization of glucosensing neuron subpopulations in the arcuate nucleus: integration in neuropeptide Y and pro-opio melanocortin networks? Diabetes 56(5):1219–1227.

[53] Jansen, A.S., Hoffman, J.L., Loewy, A.D., 1997. CNS sites involved in sympathetic and parasympathetic control of the pancreas: a viral tracing study. Brain Research 766(1—2):29—38.

[54] la Fleur, S.E., Kalsbeek, A., Wortel, J., Buijs, R.M., 2000. Polysynaptic neural pathways between the hypothalamus, including the suprachiasmatic nucleus, and the liver. Brain Research 871(1):50—56.

[55] Yi, C.X., la Fleur, S.E., Fliers, E., Kalsbeek, A., 2010. The role of the autonomic nervous liver innervation in the control of energy metabolism. Biochimica et Biophysica Acta 1802(4):416—431.

[56] Rothwell, N.J., Luheshi, G.N., 2000. Interleukin 1 in the brain: biology, pathology and therapeutic target. Trends in Neurosciences 23(12):618—625.

[57] Winkler, Z., Kuti, D., Polyak, A., Juhasz, B., Gulyas, K., Lenart, N., et al., 2019. Hypoglycemia-activated hypothalamic microglia impairs glucose counterregulatory responses. Scientific Reports 9(1):6224.

[58] McCrimmon, R.J., 2021. Consequences of recurrent hypoglycaemia on brain function in diabetes. Diabetologia 64(5):971—977.

[59] Razavi Nematollahi, L., Kitabchi, A.E., Stentz, F.B., Wan, J.Y., Larijani, B.A., Tehrani, M.M., et al., 2009. Proinflammatory cytokines in response to insulin-induced hypoglycemic stress in healthy subjects. Metabolism 58(4):443—448.

[60] del Rey, A., Besedovsky, H., 1987. Interleukin 1 affects glucose homeostasis. American Journal of Physiology 253(5 Pt 2):R794—R798.

[61] Dror, E., Dalmas, E., Meier, D.T., Wueest, S., Thevenet, J., Thienel, C., et al., 2017. Postprandial macrophage-derived IL-1beta stimulates insulin, and both synergistically promote glucose disposal and inflammation. Nature Immunology 18(3):283—292.

[62] Metzger, S., Nusair, S., Planer, D., Barash, V., Pappo, O., Shilyansky, J., et al., 2004. Inhibition of hepatic gluconeogenesis and enhanced glucose uptake contribute to the development of hypoglycemia in mice bearing interleukin-1beta- secreting tumor. Endocrinology 145(11):5150—5156.

[63] Del Rey, A., Roggero, E., Randolf, A., Mahuad, C., McCann, S., Rettori, V., et al., 2006. IL-1 resets glucose homeostasis at central levels. Proceedings of the National Academy of Sciences of the United States of America 103(43): 16039—16044.

[64] Ota, K., Wildmann, J., Ota, T., Besedovsky, H.O., Del Rey, A., 2009. Interleukin-1beta and insulin elicit different neuroendocrine responses to hypoglycemia. Annals of the New York Academy of Sciences 1153:82—88.

[65] Betley, J.N., Cao, Z.F., Ritola, K.D., Sternson, S.M., 2013. Parallel, redundant circuit organization for homeostatic control of feeding behavior. Cell 155(6): 1337—1350.

[66] Del Rey, A., Verdenhalven, M., Lörwald, A.C., Meyer, C., Hernangómez, M., Randolf, A., et al., 2016. Brain-borne IL-1 adjusts glucoregulation and provides fuel support to astrocytes and neurons in an autocrine/paracrine manner. Molecular Psychiatry 21(9):1309—1320.

[67] Véga, C., Pellerin, L., Dantzer, R., Magistretti, P.J., 2002. Long-term modulation of glucose utilization by IL-1 alpha and TNF-alpha in astrocytes: Na+ pump activity as a potential target via distinct signaling mechanisms. Glia 39(1):10—18.

[68] Minokoshi, Y., Alquier, T., Furukawa, N., Kim, Y.B., Lee, A., Xue, B., et al., 2004. AMP-kinase regulates food intake by responding to hormonal and nutrient signals in the hypothalamus. Nature 428(6982):569—574.

